Journal of Alloys and Compounds 745 (2018) 421–429

Contents lists available at ScienceDirect

Journal of Alloys and Compounds

journal homepage: http://www.elsevier.com/locate/jalcom

Preparation of tungsten carbides by reducing and carbonizing WO_2 with CO

Jie Dang*, Yijie Wu, Zepeng Lv, Xuewei Lv

College of Materials Science and Engineering, Chongqing University, Chongqing 400044, China

ARTICLE INFO

Article history:
Received 3 November 2017
Received in revised form
19 January 2018
Accepted 18 February 2018
Available online 20 February 2018

Keywords:
WO_2
Carbon monoxide
Tungsten carbides
Reduction
Carbonization

ABSTRACT

Tungsten carbides, which can be widely used as cutting and drilling tools, chemical catalysts and aerospace coatings, have attracted widespread attentions. The present work reported a simple method to prepare tungsten carbides by using WO_2 as the raw materials and CO as the reduction and carbonization agent. It was found that at lower and moderate temperatures, all the final product was WC, while at higher temperatures, the final products were W_2C or W. The reduction and carbonization mechanism was also studied theoretically and experimentally. WO_2 was reduced and carburized to WC in one step at lower temperatures; WO_2 was first reduced and carburized to W_2C and then to WC at moderate temperatures; while at higher temperatures, WO_2 was first reduced to metallic W and then carbonized to WC or W_2C, but with the temperature increasing, the carbonization became difficult and required much higher CO content.

1. Introduction

Tungsten carbides, which belong to the group of cemented carbides and refractory carbides, have advantages of high melting point, high hardness, low friction coefficients, high thermal stability and low thermal expansion coefficient[1]. These advantages make tungsten carbides appropriate for various engineering applications such as manufacture of cutting tools, rock drill tips and general wear parts[2-5]. Besides, tungsten carbides have been used as the Pt electro-catalyst support for various processes[6]. A wide variety of applications have been recognized for bulk nano-ceramics and nano-ceramic composites, for instance, the durable ceramic parts for automotive engines, ultrafine filters, aerospace erosion resistant coatings, flexible superconducting wire and fibre optic connector components[7].

Tungsten carbides mainly include two phases, namely, WC and W_2C. In general, higher tungsten carbide WC has one common structure, hexagonal structure. However, lower tungsten carbides W_2C have several structural modifications: β-W_2C, β′-W_2C, β”-$W_2C$and ε-W_2C. The presence of different types of carbon atoms distribution causes the possibility of the formation of several structural modifications of W_2C[8,9].

There are many methods for preparation of tungsten carbides. These methods include direct carburization of tungsten powder, high-energy mechanical ball milling[10], the spray conversion process[11], solid-gas reaction[12], sol-gel and in-situ carburization [13], and combustion synthesis[14]. The traditional method is to direct carburization of tungsten powders: tungsten powders are mixed with carbon black by ball-milling for an extender time, and then carbonized at 1400–1600 °C (1673–1873K)[15]. Because the tungsten powders and carbon black can not contact inadequately, the reaction proceeds slowly. The application of different sources of tungsten containing precursor and carbon-containing gas for preparation of tungsten carbides has been reported in literatures.[16,17]. These methods successfully prepared tungsten carbides. However, some of the preparation processes can be complicated. Because in these processes, a special precursor must be prepared before reduction and carbonization, such as the coating of precursor with carbon. Table 1 summarized the typical specific methods which were reported in the literatures, for preparation of WC. In all of the specific methods of preparation of tungsten carbide, the processes required either a higher temperature or a long time. Venables and Brown[22] studied the reduction of WO_3 with CO, which showed that the reaction temperature can be reduced.

The aim of this work is to prepare tungsten carbides by using WO_2 as the raw materials and CO as the reduction and carbonization agent. The reduction and carbonization mechanisms were

* Corresponding author.
E-mail address: jiedang@cqu.edu.cn (J. Dang).

https://doi.org/10.1016/j.jallcom.2018.02.224
0925-8388/

studied theoretically and experimentally as well.

2. Material and experimental

WO_2 powders (larger than 100 mesh, 99.9% metals basis) from Aladdin Industrial Corporation were employed as the raw material. Co powders (40–100 mesh, 99.9% metals basis) from Chengdu Jinchun metal material Co., Ltd. were also used as raw materials.

An HCT-2 Thermo-Gravimetric Analyzer (TGA) was used to monitor the weight change of samples during reduction and the experimental apparatus was described elsewhere. [23] A sample of around 100 mg was used in each experimental run and after an alumina crucible (8 × 8mm) with samples was put into the TGA, high-purity argon was introduced to flush air out of the furnace. In isothermal reduction, the furnace was first heated from room temperature up to a desired reduction temperature at a rate of 10 °C/min while maintaining the argon atmosphere. Once the thermal balance stabilized, the argon gas was switched to reaction gas, and the weight loss was then monitored continuously by the TGA. After reacting for a certain time, the reaction gas was switched to argon again, and samples were cooled down to room temperature. In non-isothermal experiments, CO was first used to flush air from the furnace, and then the furnace was heated from room temperature to 1200 °C at heating rates of 4, 6 and 8 K/min, in different runs. In all experimental runs, a constant gas flow rate of 60 ml/min (about 0.318×10^{-2} m/s at 25 °C) was maintained. The flow rate of gas was controlled by gas flow controllers (Alicant, Model MC-500SCCM-D).

To study the mechanical performance of the prepared WC, WC-6 wt% Co composites were prepared using the hot-press sintering technique. Around 10 g WC powders and Co powders (with mass fraction of 6%) were mixed first and then pressed into cylinder under an axial mechanical pressure of 11 MPa. The hot pressing was processed in high strength graphite die, high purity argon gas under an axial mechanical pressure of 13 MPa at 1500 °C for 3 h.

X-Ray Diffraction (XRD) (PANalytical X'Pert Powder, Panalytical B.V.) measurements were conducted for samples. Morphologies of these samples were observed using SEM (TESCAN VEGA 3 LMH, Czech Republic) technique. The Brunauer– Emmett–Teller (BET) method was employed to determine the surface areas of samples at 77 K (Micromeritics ASAP 2020, American). The hardness of WC-6 wt% Co composites sample was determined using hardometer (Hengyi MH-6, China). The thermodynamics calculations were performed by using FactSage 6.2 with pure substances database.

3. Expected reactions

Equilibrium calculations were carried out for an indication of the expected reactions during the reduction and carburization. Fig. 1 gives the equilibrium diagram of CO and WO_2 system, which clearly shows the reaction products at different temperatures and $CO/(CO + WO_2)$ ratios. It can be obtained that at low temperatures, WC is the most stable phase, but W_2C and W would be formed with increasing the temperature, and the ratio of $CO/(CO + WO_2)$ must be rather close to 1 to form W_2C and WC at high temperatures. Figs. 2 and 3 give the calculated results for three typical experimentally used temperatures: 813 °C (1086 K), 908 °C (1181 K) and 1179 °C (1452 K). Fig. 2 shows the W–O–C predominance diagrams (for the three temperatures). The line of crosses in Fig. 2 represents a total gas pressure of 1 atm; equilibrium gas compositions (consisting largely of CO and CO_2) would lie along this line if WO_2 was to react with pure CO in different molar ratios, for a total pressure of 1 atm. The formation of WC would require a more CO-rich gas, corresponding to gas compositions towards the lower right in the predominance diagrams (along the lines of crosses). Fig. 2 indicates

Table 1
Different methods for preparation of WC in literatures.

Preparation methods	Reaction temperature	Time	Tungsten contain precursor	Carbon source
Direct carburization[15]	$W + C \xrightarrow{\text{ball milling}} W + C \xrightarrow{H2/1400\sim1600^{\circ}C} WC$	Ball milling: 20 h Reaction: 2–10 h	Tungsten powder	Carbon black
High energy mechanical ball milling[18]	$W + C \xrightarrow{\text{ball milling}} W + C \xrightarrow{H2/1000^{\circ}C} WC$	Mixing Ball milling: 90 h Reaction: 1 h	Tungsten powder	Activated granular carbon
Spray conversion process[11,19]	$APT \xrightarrow[2.5\sim3.5\ MPa]{\text{spray drying at } 250\sim350^{\circ}C,} WO_3 WO_3 \xrightarrow{420\sim500^{\circ}C} WO_{2.9} WO_{2.9} \xrightarrow{700\sim740^{\circ}C} W\ powder \xrightarrow{980\sim1000^{\circ}C} WC$	$(WO_3 \rightarrow WO_{2.9})$ Reaction: 1.2 h $(WO_{2.9} \rightarrow W)$ Reaction: 1.5 h $(W \rightarrow WC)$ Reaction: 1.5 h	Ammonium tungstate(APT)	Carbon black; Phenolic resin; Industrial alcohol
The vapor phase reaction[20]	$WCl_6 + H_2 \xrightarrow{400^{\circ}C} WW + CH_4 \xrightarrow{H2/1400^{\circ}C} WC$	Carburization: over 2 h	Tungsten hexachloride (WCl_6)	$CH_4 + H_2$
Sol-Gel preparation method[21]	$\text{Ammonium polyacrylic} + \text{water} + Na_2WO_4 \xrightarrow{\text{Saturated hexanol+HC}} \text{precipitation of tungstic acid} \xrightarrow[\text{drying at } 120^{\circ}C]{} \text{the dry gel} \xrightarrow[(1)\ Ar/900^{\circ}C,\ (2)\ CO2/900^{\circ}C]{} WC$	Drying: 12 h Calcine: 4 h	Sodium tungstate HCl Hexanol	Ammonium polyacrylate; CO_2

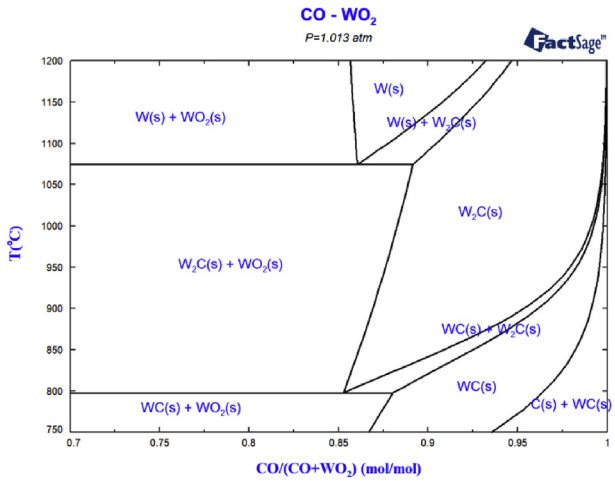

Fig. 1. Equilibrium diagram showing solid phase fields as a function of temperature and input CO mole fraction in theWO_2-CO system.

that different reaction sequences should be expected for reaction at higher and lower temperatures. At the lower temperatures (813 °C and 908 °C in this example), WO_2 can be simultaneously reduced and carburized, but first forming W_2C and then forming WC, according to reaction (1a) and (1b):

$$2WO_2 + 6CO = W_2C + 5CO_2 \quad (1a)$$

$$W_2C + 2CO = 2WC + CO_2 \quad (1b)$$

However, at the higher temperature, WO_2 would be reduced to W first, followed by carburization to form W_2C, and even WC at much higher CO/CO_2 ratios, according to the three steps of reaction (2):

$$2WO_2 + 4CO = 2W + 4CO_2 \quad (2a)$$

$$2W + 2CO = W_2C + CO_2 \quad (2b)$$

$$W_2C + 2CO = 2WC + CO_2 \quad (2c)$$

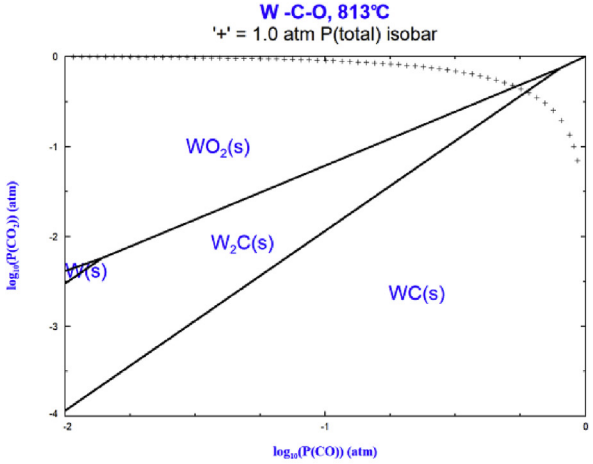

(a)

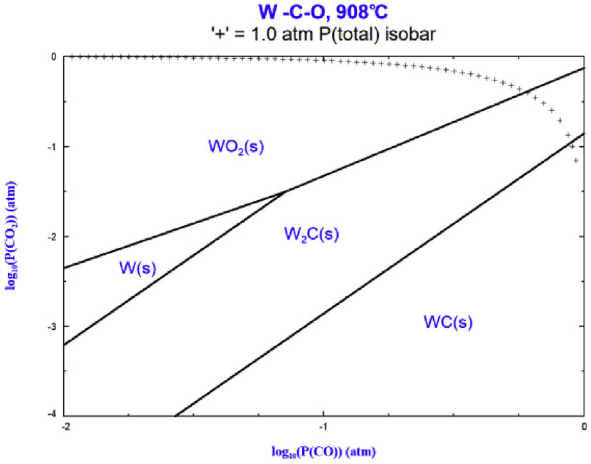

(b)

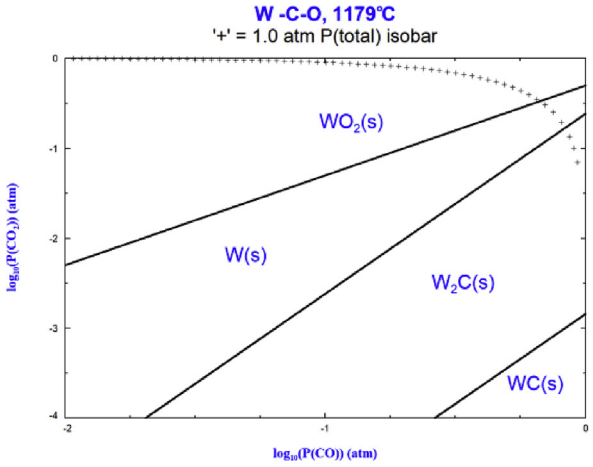

(c)

Fig. 2. Predominance diagrams for reduction and carburization of WO_2 by reaction with CO at 813 °C, 908 °C and 1179 °C, total gas pressure of 1 atm given by crosses (+).

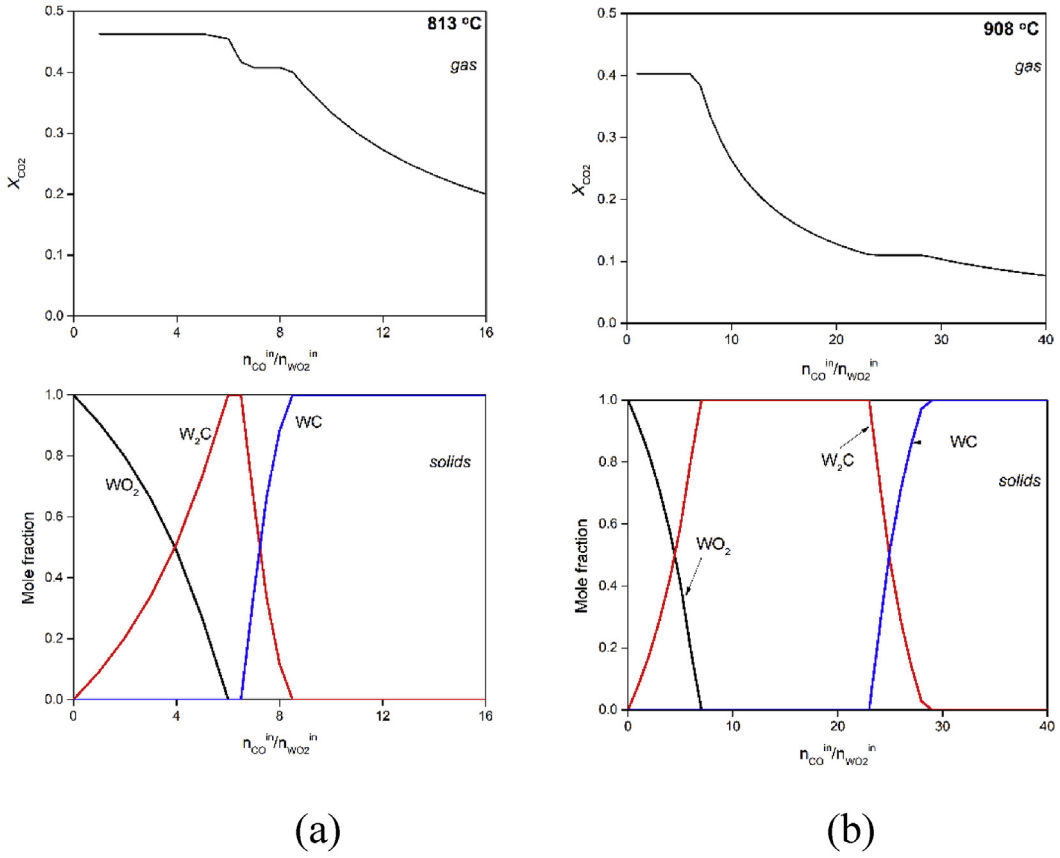

Fig. 3. Stable gaseous and solid reaction products after equilibration of different molar ratios of WO_2 and CO at 813 °C, 908 °C and 1179 °C. (1 atm total pressure).

This difference in expected reaction sequence is also illustrated by Fig. 3, which shows the equilibrium reaction products for reaction of WO_2 and CO in different molar ratios. In Fig. 3, the partial pressure of CO_2 - balance is CO - is shown in the upper graphs; the relative molar amounts of solid phases are shown in the lower graphs. Fig. 3 confirms the difference in expected reaction sequence: simultaneous reduction and carburization [reaction (1)] at the lower temperature, and reduction to W, followed by carburization to W_2C at the higher temperature [reaction (2)]. However, it should be noted that the final product is W_2C at 1179 °C even the ratio of n^{in}_{CO}/n^{in}_{WO2} is as much as 40 or even higher. Fig. 3 also illustrates that the CO_2 partial pressure required to yield W_2C as stable product is much lower at the higher temperature.

These predicted reaction sequences were tested experimentally by measuring the phases in partially reduced materials, and by monitoring the mass loss during reaction (thermogravimetry). The difference in mass loss for the different reaction sequences was readily detectable: completion of reaction (1) (reduction and carburization, forming WC) would give a reduction in mass of the solid of 9.27% (relative to the original mass of WO_2) and completion of reaction (1a) to form W_2C would give a mass loss of 12.05%, whereas completion of reaction (2a) (reduction to W) would give a mass loss of 14.83%.

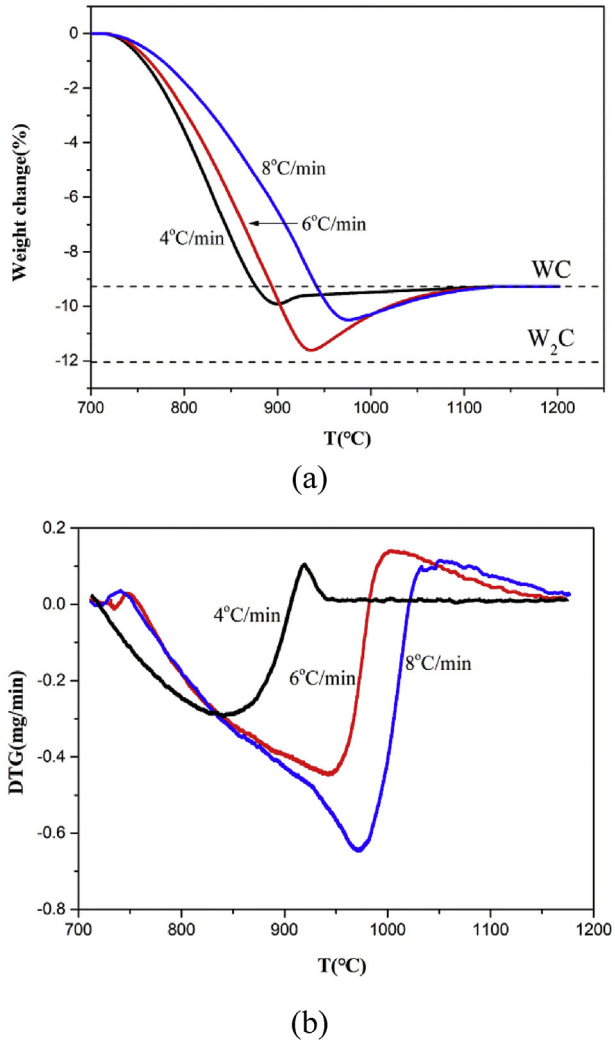

Fig. 4. Non-isothermal reduction of WO_2 with pure CO: (a) weight change verse temperature, (b) DTG verse temperature.

4. Results and discussion

4.1. Non-isothermal reaction

To clarify the onset temperature of reduction and the effect of ramping rates on the reaction, non-isothermal reduction of WO_2 powders was performed by using pure carbon monoxide at three different ramping rates, 4 °C/min, 6 °C/min and 8 °C/min. The obtained results are shown as Fig. 4. Fig. 4a shows the temperature dependences of the weight changes during non-isothermal reaction, which demonstrates that different ramping rates have a significant effect on the reduction rate and the reaction route. It is shown that the reaction became apparent at around 730 °C (1003 K), and a higher heating rate led to a faster reaction (Fig. 4b). Based on the weight change, the reaction is divided into two steps, loss-mass reaction and gain-mass reaction. All the three curves first go over −9.27% (corresponding to forming WC) but do not reach −12.05% (corresponding to forming W_2C), and then go back to −9.27%. It suggests that only part of WO_2 was first reduced and carbonized to W_2C and then to WC, which is confirmed by XRD analysis (listed in Table 2). This is because at low temperature, WC is formed directly, but with increasing the temperature, W_2C will be formed first. With increasing the ramping rate from 4 °C/min to 6 °C/min, the amount of formed W_2C increases dramatically, resulting from the rapid approaching W_2C forming temperature; while increasing the ramping rate to 8 °C/min, the amount of W_2C drops off, which may be caused by reacting formed W_2C to WC immediately at high temperature.

The maximum rate for the first reaction (loss-mass reaction) appeared at 840 °C (1113 K), 945 °C (1218 K), and 973 °C (1246 K) at the heating rate of 4 °C/min, 6 °C/min and 8 °C/min (Fig. 4b), respectively. The slow reaction rates at low temperatures and high temperatures are due to the relatively small reduction rate constant and the exhaustion of samples, respectively. The highest reduction rate has occurred at the temperature when both reduction rate constant and oxide concentration were at the high levels.

4.2. Isothermal reaction

Isothermal reduction of WO_2 by pure CO was studied in the temperature range of 813 °C (1086 K) to 1179 °C (1452 K). Fig. 5 shows the time dependences of the weight changes during isothermal reduction at eight different temperatures. The figure shows that at lower temperatures [below 861 °C (1134 K)], the mass loss increased smoothly to 9.27% (corresponding to the weight change from WO_2 to WC); at moderate temperatures [884 °C (1157 K) to 908 °C (1181 K)], the weight loss ratio first increased over 9.27% but not up to 12.05% (corresponding to the weight change from WO_2 to W_2C), and finally decreased to 9.27%; at 1009 °C (1282 K) and 1102 °C (1375 K), the weight loss ratio first increased up to 14.83% (corresponding to the weight change from WO_2 to W) and then decreased to about 9.27%; however, the weight loss ratio first increased up to 14.83% and then decreased very slow when the reaction proceeded at 1150 °C (1423 K) and 1179 °C (1452 K). This reaction behavior is consistent with the expected reaction sequence, as discussed earlier: at lower temperatures, simultaneous reduction and carburization to form WC directly from WO_2 is expected; at the moderate temperatures, two-step reduction and carburization in WO_2 to W_2C, followed by further carburization of W_2C to form WC are expected; while at high temperature, reduction of WO_2 to W and then carburization of W to WC are expected; at even higher temperatures, W_2C as the most stable phase is expected, however, the carburization proceeds very slow.

XRD analyses for completely reduced samples at 813 °C

Table 2
Phase compositions of samples reduced under different conditions (based on XRD analyses).

Reduction of WO_2 by CO under different conditions	Phases composition		
	major	minor	trace
Non-isothermal reduction (ramping rate of 4 °C/min)	WC	–	–
1179 °C for 222min (isothermal reduction)	W	–	W_2C
1102 °C for 175min (isothermal reduction)	WC	W	W_2C
813 °C for 30 min (isothermal reduction)	WO_2	–	WC; β"-W_2C
1009 °C for 47 min (isothermal reduction)	W	–	–

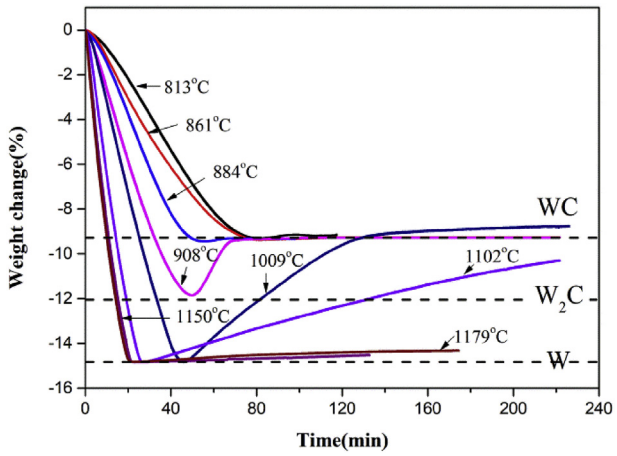

Fig. 5. Reduction curves of WO_2 by pure CO at different temperatures.

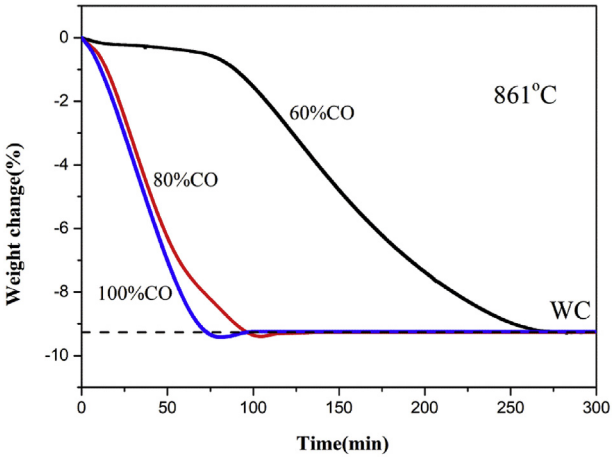

Fig. 7. The effect of CO content on the reduction of WO_2 at 861 °C.

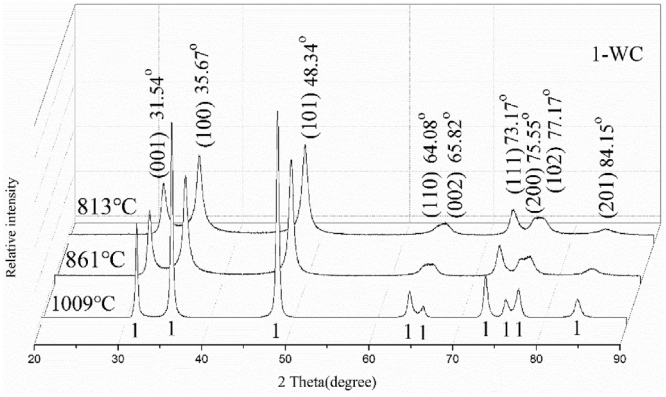

Fig. 6. XRD patterns of completed reduction of WO_2 by CO at 813 °C, 861 °C and 1009 °C.

(1086 K), 861 °C (1134 K) and 1009 °C (1282 K) are shown as Fig. 6, which confirms that the final product is WC for samples of which the mass loss is around 9.27% after reaction. It should be noted that higher temperature results in better crystallization. The phase's compositions of samples reduced at 1102 °C (1375 K) for 175min and 1179 °C (1452 K) for 222min were also detected (Table 2). It shows that at 1179 °C (1452 K), the final products are almost W with trace amount of W_2C. Combining the TG curves (Fig. 5), it can be obtained that at higher temperature [above 1150 °C (1423 K)], the formation of W_2C or WC is very difficult and requires higher CO content, which agrees well with the thermodynamics results (Figs. 1 and 2). To confirm the reduction process, X-ray diffraction detections of samples partially reacted at 813 °C (1086 K) and 1009 °C (1282 K) were carried out and the obtained phase compositions are shown in Table 2. It illustrates the difference in reaction sequence depending on temperature: at 813 °C (1086 K) the reduction sequence is WO_2 to β"-W_2C and then to WC, which is consistent with the thermodynamics calculations (Figs. 2 and 3), and the reactions of WO_2 to W_2C and W_2C to WC occurred simultaneously; while in the sample reduced for 47 min at 1009 °C (1282 K) (corresponding to the lowest point of TG curve for 1009 °C), only W phase was detected, in agreement with the expectation that at higher temperatures WO_2 would first be reduced to metallic W.

4.3. The effect of CO content on the reaction

The effect of CO content on the reduction of WO_2 was investigated in this study as well. Fig. 7 shows the time dependences of the weight changes in reduction of WO_2 with different CO content 861 °C (1134 K). It can be obtained that CO content has a significant influence on the reduction and carbonization rate. With increasing the CO content from 60% to 80%, the reduction and carbonization rate increases greatly, but from 80% to 100%, the reduction and carbonization rate has a modest rise.

4.4. Morphology of reacted samples

Fig. 8 shows the SEM images of samples completely or partially reacted at different temperatures. The morphologies of WC obtained at low and high temperatures are quite different: at 813 °C (1086 K), the obtained WC particles show acicular shape (Fig. 8a); while full reaction at 1009 °C (1282 K) results in WC particles with spherical shape (Fig. 8d), which retains the spherical shape of the

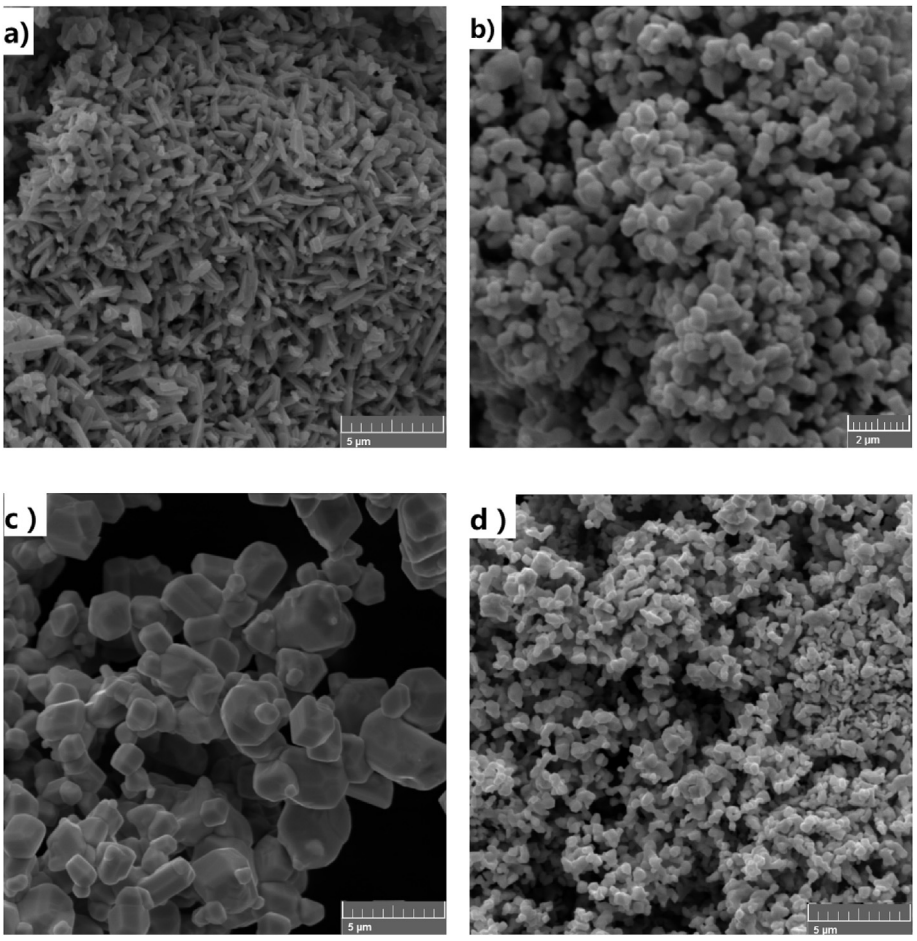

Fig. 8. SEM images of: (a) sample completely reduced at 813 °C (WC); (b) sample reduced at 1009 °C for 47min (W); (c) sample reduced at 1179 °C for 222 min (W with trace amount of W_2C); (d) sample completely reduced at 1009 °C (WC).

W particles (Fig. 8b). Fig. 8b and d indicate that the fine substructure forms during initial reduction in WO_2 to W, not during subsequent carburization. Fig. 8c represents the SEM image of W particles produced at 1179 °C (1452 K). Comparing with W produced at 813 °C (1086 K) (Fig. 8b), W particles produced at 1179 °C (1452 K) are larger and show a quite different shape (largely polyhedron). Fig. 9 shows the typical TEM images of raw WO_2 and WC powders obtained at different temperatures. Fig. 9A1 and B1 clearly show that the morphologies of raw WO_2 and WC obtained at 813 °C are acicular shaped and the particle sizes of them are nearly the same as each other, which are well agreement with the images obtained by the SEM (Fig. 8). That means WC obtained at 813 °C inherited the morphology of the raw material WO_2. However, Fig. 9C1 demonstrates that the shape and size of WC prepared at 1009 °C are quite different from those of WC obtained at 813 °C, and the WC obtained at 1009 °C are polyhedron shaped. The corresponding SAED patterns for these specimens are depicted in Fig. 9A2, B2 and C2, respectively. The diffraction spots are exhibited for WO_2 and WC prepared at 1009 °C, which suggests that WO_2 and WC prepared at 1009 °C are both single-crystalline structure. Although the diffraction rings shown in Fig. 9B2 are not very perfect, WC prepared at 1009 °C has a polycrystalline structure can be confirmed. The BET surface areas (average mesopore size in parenthesis) were 1.8965 m^2/g (7.657 nm) for WC obtained at 813 °C, 7.5051 m^2/g (12.219 nm) for that obtained at 861 °C, and 10.3442 m^2/g (11.391 nm) for that obtained at 1009 °C, and the calculated particle sizes are 202.4 nm, 51.1 nm and 37.1 nm, respectively.

The surface areas of WC obtained in this study are similar to those obtained by Ma et al.[24] via direct solid-state synthesis from mechanically activated tungsten oxide and graphite and Won et al.[14] by combustion synthesis.

4.5. Hardness of WC-6 wt% Co composites

The prepared WC obtained at 813 °C was used to check its property. WC-6 wt% Co composites were prepared using the hot-press sintering technique. The determined hardness of WC-6 wt% Co composites is 1748.8 kgf/mm^2 (HV), which is in the range of those reported in the literatures [25,26].

5. Conclusions

In this study, a method to prepare tungsten carbides was reported. The precursor used to produce tungsten carbides was WO_2, and the reduction and carbonization agent was CO. Based on the thermodynamic analyses and experiments, the reduction and carbonization mechanisms were obtained: at lower temperatures,

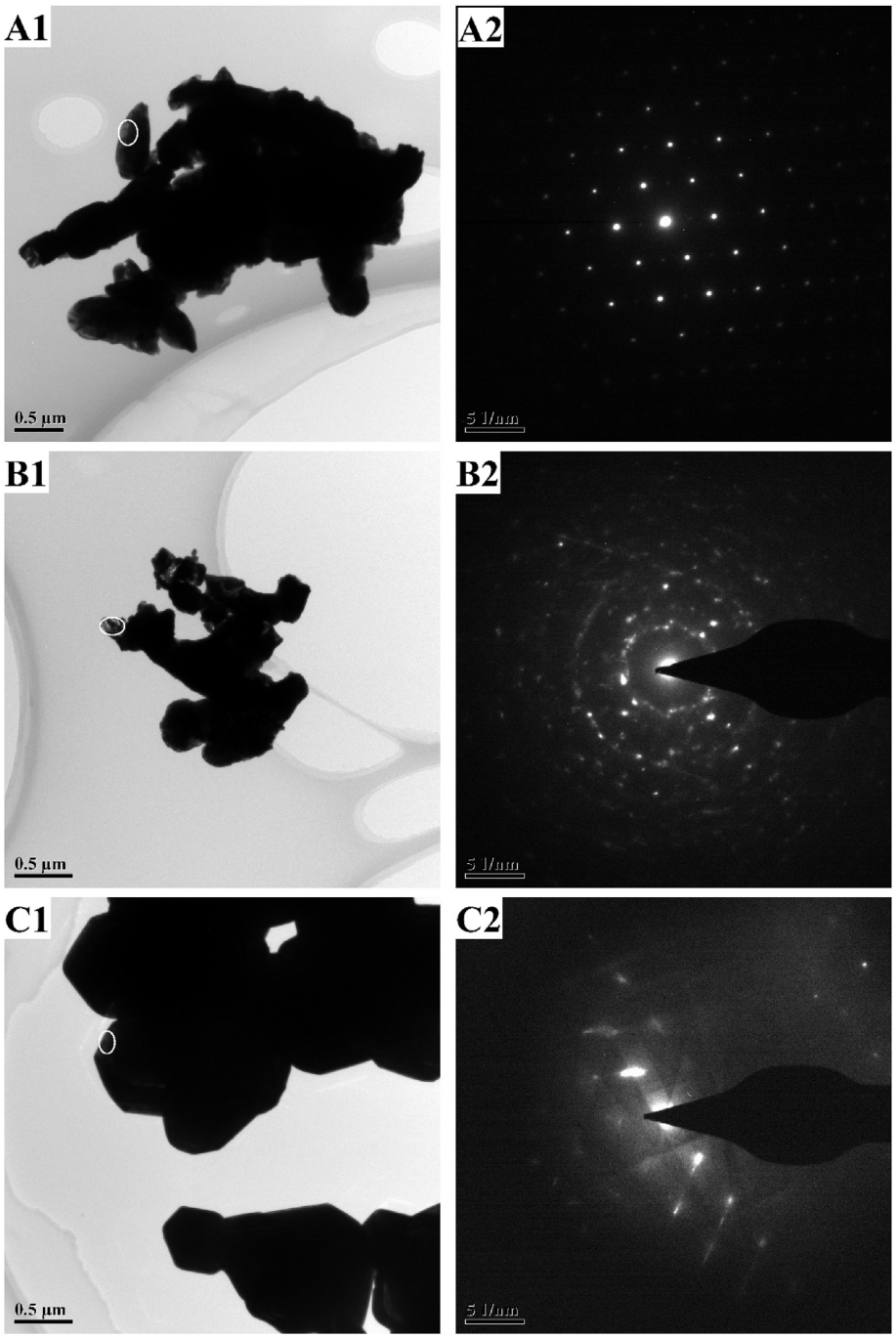

Fig. 9. Typical TEM images of the particles; A1: raw WO_2 powders, B1: sample completely reduced at 813 °C (WC), C1: sample completely reduced at 1009 °C (WC). A2, B2 and C2 are the SAED patterns recorded from the ellipses marked in A1, B1 and C1, respectively.

WO_2 was reduced and carburized to WC in one step; at moderate temperatures, WO_2 was first reduced and carburized to W_2C and then to WC; while at higher temperatures, WO_2 was first reduced to metallic W and then carbonized to WC or W_2C, but with the temperature increasing, the carbonization became difficult and required much higher CO content. The morphologies of samples reduced and carbonized were also investigated and it was found that the morphologies of WC prepared at different temperatures were quite different.

Acknowledgements

Thanks are given to the financial supports from the National Natural Science Foundation of China (51604046, 51674053), Fundamental and Frontier Research Project of Chongqing (cstc2017jcyjAX0322), State Key Laboratory of Advanced Metallurgy (KF-17-02), and the Fundamental Research Funds for the Central Universities (106112016CDJXY130005 and 106112017CDJXY130002).

References

[1] T.I.A. Kosolapova, Carbides: properties, production, and applications, Chem. Commun. 49 (1971) 11133–11148.
[2] V. Bounhoure, S. Lay, M. Loubradou, J.M. Missiaen, Special WC/Co orientation relationships at basal facets of WC grains in WC-Co alloys, J. Mater. Sci. 43 (2008) 892–899.
[3] M. Sternitzke, Review: structural ceramic nanocomposites, J. Eur. Ceram. Soc. 17 (1997) 1061–1082.
[4] K. Jia, T.E. Fischer, B. Gallois, Microstructure, hardness and toughness of nanostructured and conventional WC-Co composites, Nanostruct. Mater. 10 (1998) 875–891.
[5] W.D. Schubert, A. Bock, B. Lux, General aspects and limits of conventional ultrafine WC powder manufacture and hard metal production, Int. J. Refract. Met. Hard Mater. 13 (1995) 281–296.
[6] S. Bukola, B. Merzougui, A. Akinpelu, M. Zeama, Cobalt and nitrogen Co-doped tungsten carbide catalyst for oxygen reduction and hydrogen evolution reactions, Electrochim. Acta 190 (2016) 1113–1123.
[7] D. Garg, P.N. Dyer, Tungsten carbide erosion resistant coating for aerospace components, Mater. Res. Soc. Symp. Proc. 168 (1989) 213.
[8] A. Harsta, A. Rundqvist, J.O. Thomas, A neutron powder diffraction study of W_2C, Acta Chem. Scand 32a (1978) 891–892.
[9] A.S. Kurlov, A.I. Gusev, Tungsten carbides: structure, properties and application in hard metals, Springer Ser. Mater. Sci. 184 (2013) 5–25.
[10] H.J. Fecht, E. Hellstern, Z. Fu, W.L. Johnson, Nanocrystalline metals prepared by high-energy ball milling, Metall. Trans. A 21 (9) (1990) 2333.
[11] L.E. Mccandlish, B.H. Kear, S.J. Bhatia, Spray conversion process for the production of nanophase composite powders, US Patent No:5352269 A, 1994.
[12] F.F.P. Medeiros, S.A.D. Oliveira, C.P.D. Souza, A.G.P.D. Silva, U.U. Gomes, J.F.D. Souza, Synthesis of tungsten carbide through gas-solid reaction at low temperatures, Mater. Sci. Eng. A 315 (2001) 58–62.
[13] C. Giordano, M. Antonietti, Synthesis of crystalline metal nitride and metal carbide nanostructures by sol-gel chemistry, Nano Today 6 (2011) 366–380.
[14] H.I. Won, H.H. Nersisyan, C.W. Won, Combustion synthesis of nano-sized tungsten carbide powder and effects of sodium halides, J. Nanopart. Res. 12 (2010) 493–500.
[15] L.E. Toth, Transition Metal Carbides and Nitrides, 320, Academic Press, 1971, 12069–12073(5).
[16] R. Koc, S.K. Kodambaka, Tungsten carbide (WC) synthesis from novel precursors, J. Eur. Ceram. Soc. 20 (2000) 1859–1869.
[17] S. Decker, A. Löfberg, J.M. Bastin, A. Frennet, Study of the preparation of bulk tungsten carbide catalysts with C_2H_6/H_2 and C_2H_4 /H_2 carburizing mixtures, Catal. Lett. 44 (1997) 229–239.
[18] G.M. Wang, S.J. Campbell, A. Calka, W.A. Kaczmarek, Synthesis and structural evolution of tungsten carbide prepared by ball milling, J. Mater. Sci. 32 (6) (1997) 1461–1467.
[19] C.Y. Wu, L.Y. Zhang, A method to prepare nanoparticles of tungsten and tungsten carbide, CN Patent No:1608983A. 2005.
[20] J. Hojo, T. Oku, A. Kato, Tungsten carbide powders produced by the vapor phase reaction of the WCl_4-CH_4-H_4 system, J. Less-Common Metals 59 (1) (1978) 85–95.
[21] M.J. Hudson, J.W. Peckett, P.J.F. Harris, Low-temperature sol-gel preparation of ordered nanoparticles of tungsten carbide/oxide, Ind. Eng. Chem. Res. 44 (2005) 5575–5578.
[22] D.S. Venables, M.E. Brown, Reduction of tungsten oxides with carbon monoxide, Thermochim. Acta 291 (1997) 131–140.
[23] J. Dang, G.H. Zhang, K.C. Chou, Study on kinetics of hydrogen reduction of MoO_2, Int. J. Refract. Met. Hard Mater. 41 (2013) 356–362.
[24] J. Ma, S.G. Zhu, Direct solid-state synthesis of tungsten carbide nanoparticles from mechanically activated tungsten oxide and graphite, Int. J. Refract. Met. Hard Mater. 28 (2010) 623–627.
[25] Y.V. Milman, S. Chugunova, V. Goncharuck, Low and high temperature hardness of WC-6 wt%Co alloys, Int. J. Refract. Met. Hard Mater. 15 (1997) 97–101.
[26] Z.Z. Fang, X. Wang, T. Ryu, K.S. Kwang, H.Y. Sohn, Synthesis, sintering, and mechanical properties of nanocrystalline cemented tungsten carbide–A review, Int. J. Refract. Met. Hard Mater. 27 (2009) 288–299.